

## Single domain Bi<sub>2</sub>Se<sub>3</sub> films grown on InP(111)A by molecular-beam epitaxy

X. Guo,<sup>1</sup> Z. J. Xu,<sup>1</sup> H. C. Liu,<sup>2</sup> B. Zhao,<sup>3</sup> X. Q. Dai,<sup>3,4</sup> H. T. He,<sup>2,5</sup> J. N. Wang,<sup>2</sup> H. J. Liu,<sup>1</sup> W. K. Ho,<sup>1</sup> and M. H. Xie<sup>1,a)</sup>

<sup>1</sup>Department of Physics, The University of Hong Kong, Pokfulam Road, Hong Kong

<sup>2</sup>Department of Physics, Hong Kong University of Science and Technology, Clear Water Bay, Kowloon, Hong Kong

<sup>3</sup>College of Physics and Information Engineering, Henan Normal University, Xinxiang, Henan 453007, China

<sup>4</sup>Department of Physics, Zhengzhou Normal University, Zhengzhou, Henan 450044, China

<sup>5</sup>Department of Physics, South University of Science and Technology of China, Shenzhen, China

(Received 4 December 2012; accepted 9 April 2013; published online 19 April 2013)

We report the growth of single-domain epitaxial Bi<sub>2</sub>Se<sub>3</sub> films on InP(111)A substrate by molecular-beam epitaxy. Nucleation of Bi<sub>2</sub>Se<sub>3</sub> proceeds at steps, so the lattices of the substrate play the guiding role for a unidirectional crystalline film in the step-flow growth mode. There exists a strong chemical interaction between atoms at the heterointerface, so the growth does not follow the van der Waals epitaxy process. A mounded morphology of thick Bi<sub>2</sub>Se<sub>3</sub> epilayers suggests a growth kinetics dictated by the Ehrlich-Schwoebel barrier. The Schubnikov de Haas oscillations observed in magnetoresistance measurements are attributed to Landau quantization of the bulk states of electrons. © 2013 AIP Publishing LLC [<http://dx.doi.org/10.1063/1.4802797>]

Bi<sub>2</sub>Se<sub>3</sub> is a three-dimensional topological insulator (TI), which has been studied extensively in recent years.<sup>1,2</sup> In the interest of better samples, efforts have been made to grow high quality Bi<sub>2</sub>Se<sub>3</sub> epilayers on many different substrates.<sup>3–11</sup> Despite Bi<sub>2</sub>Se<sub>3</sub> growth is found to be tolerant to the choice of the substrates, the structural quality of Bi<sub>2</sub>Se<sub>3</sub> epilayer does show a dependence on the characteristics of the substrate, where an inert and closely lattice-matched substrate appears favorable for better epitaxial Bi<sub>2</sub>Se<sub>3</sub> thin films.<sup>12</sup>

In this study, we experiment Bi<sub>2</sub>Se<sub>3</sub> growth on InP(111)A (i.e., indium (In) terminated) substrate by molecular-beam epitaxy (MBE). InP is a common III-V semiconductor which has a lattice parameter closely matches that of Bi<sub>2</sub>Se<sub>3</sub> in the *c*-plane (e.g., the spacing between the nearest neighbor In atoms in the (111) plane of InP is ~0.415 nm while that between Se atoms of Bi<sub>2</sub>Se<sub>3</sub> is ~0.414 nm). Therefore, MBE growth of Bi<sub>2</sub>Se<sub>3</sub> along the *c*-axis on InP(111) represents a lattice-matched heteroepitaxial system. There are already reports of Bi<sub>2</sub>Se<sub>3</sub> growth on InP(111)B, revealing improved epitaxial quality. For example, Takagaki and Jenichen obtained smooth Bi<sub>2</sub>Se<sub>3</sub> films in a hot-wall epitaxy and noted a fixed in-plane orientation relation between the epifilm and the substrate.<sup>13</sup> Tarakina *et al.* made a comparison between Bi<sub>2</sub>Se<sub>3</sub> growth on Si(111) versus that on InP(111)B and observed much improved film quality for the latter.<sup>14</sup> By transmission electron microscopy (TEM) studies, they also revealed the presence of poor interface layers, which might be responsible for the rotation and twin domains in their films.<sup>14</sup> More recently, Schreyeck *et al.* reported growth of high quality Bi<sub>2</sub>Se<sub>3</sub> epifilm on InP(111)B by MBE, revealing low mosaicity-tilt and -twist in the epifilm. However, twin-domain were seen to persist.<sup>15</sup> Here we follow the initial stage nucleation of Bi<sub>2</sub>Se<sub>3</sub> on InP(111)A and reveal the role played by surface steps in guiding in-plane lattices of Bi<sub>2</sub>Se<sub>3</sub>. Rotation and twin domains are effectively diminished in samples grown on

InP(111)A via the step-flow growth process. Total energy calculations show strong chemical interaction between In and Se atoms at the heterointerface; therefore, the system does not follow the process of van der Waals epitaxy (vdWe).<sup>16,17</sup> The grown single-domain epifilms show reduced background doping and enhanced electron mobility. Magnetoresistance (MR) measurements also reveal the Schubnikov de Haas (SdH) oscillations that are attributed to bulk state Landau quantization.

Bi<sub>2</sub>Se<sub>3</sub> MBE growth and subsequent surface analyses using reflection high-energy electron diffraction (RHEED), low energy electron diffraction (LEED), and scanning tunneling microscopy (STM) were carried out in a customized Omicron ultrahigh vacuum (UHV) system. In the MBE chamber, conventional Knudsen cells were used for both Bi and Se sources, and their fluxes were  $1.8 \times 10^{13}$  atoms/cm<sup>2</sup>s and  $2.7 \times 10^{14}$  atoms/cm<sup>2</sup>s, respectively, during deposition. The film growth rate was about 0.76 nm/min. Singular and vicinal (3.5° offcut toward  $[\bar{1}\bar{1}2]$ ) InP (111)A substrates were deoxidized at 620 K until the (1 × 1) streaky RHEED pattern emerged, after which Bi<sub>2</sub>Se<sub>3</sub> deposition was carried out at 450 K. After a desired coverage, the growth was stopped, and the sample was then transferred under UHV to adjacent chambers for the LEED and STM characterizations. For some samples without any capping layer, transport measurements were performed using the Hall bar geometry in a Quantum Design Physical Property Measurement System (PPMS) at temperatures varying between 2 K and room temperature (RT). The Hall bars were fabricated by the standard photolithography technique with the dimension between two voltage probes of 200 μm long and 100 μm wide. The ohmic electrodes of the Hall bars were formed by thermal evaporation of Cr (20 nm)/Au (180 nm) layers.

Figure 1(a) depicts a typical RHEED pattern taken along InP[1 $\bar{1}$ 0] during Bi<sub>2</sub>Se<sub>3</sub> deposition on a singular InP(111)A substrate, where the sharp and streaky diffraction patterns are seen to persist over the entire deposition period. It suggests a

<sup>a)</sup>Email: mhxie@hku.hk

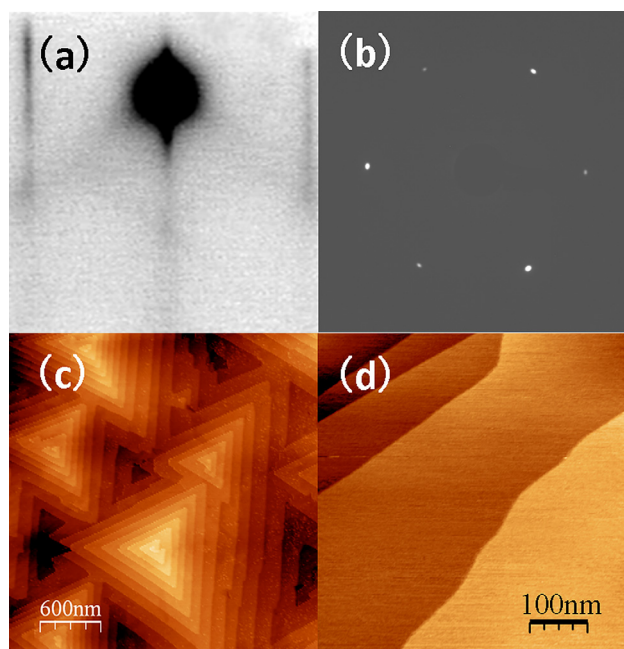


FIG. 1. (a) RHEED and (b) LEED patterns, taken at 10 keV and 30 eV respectively, from an epitaxial  $\text{Bi}_2\text{Se}_3$  on singular InP(111) substrate. Note the 3-fold symmetry pattern in (b) and asymmetrical RHEED streaks in (a), signaling a single domain epilayer. STM micrographs at different magnifications of the same sample, showing the wedding cake mounds pointed along the same direction (c) and large terraces composing the sidewalls of the mounds.

two dimensional (2D) growth mode. On a very flat substrate surface, depositing  $\text{Bi}_2\text{Se}_3$  at a reduced temperature leads to the RHEED intensity oscillations as exemplified in the inset of Figure 3(a). Such RHEED oscillations imply the 2D island nucleation growth mode. On the other hand, on a surface containing a high density of steps and depositing  $\text{Bi}_2\text{Se}_3$  at elevated temperatures, the RHEED intensity ceases to oscillate, while the diffraction pattern remains streaky. This indicates the so-called step-flow growth mode where all of the deposits incorporate in the film at step edges. In this latter situation, we obtain films that are diminished of rotation and twin domains, which are manifested by the three-fold symmetrical LEED patterns as shown in Figure 1(b) and by the unidirectional mounds seen by STM in Figure 1(c). As is discussed in detail in Ref. 18 and noted for  $\text{Bi}_2\text{Se}_3$  growth,<sup>4,19</sup> the anisotropic growth rates of steps on a hexagonal crystal surface would lead to triangular islands instead of hexagonal ones. Based on the orientation of the triangular islands or mounds, one may infer the crystallographic domain of the epifilm. If a film contains rotation or twin domains, the surface would show oppositely oriented triangular islands.<sup>4,12</sup> On the other hand, if the film is of single domain, the islands will all align in the same direction as exemplified in Figure 1(c). The single domain film correspondingly gives rise to a LEED pattern that is three-fold in symmetry, whereas a twinned film would give rise to a six-fold LEED pattern. So based on the results of Fig. 1, we assert that a single-domain  $\text{Bi}_2\text{Se}_3$  epilayer has been obtained by MBE on InP(111)A. Our LEED has a spot size of  $\sim 0.5$  mm in diameter, so the alignment of the lattice would at least extend over a similar length scale. In fact, we have repeated the LEED experiment at different locations of samples all showed the three-fold symmetry. This marks a

significant improvement over films grown on some other substrates such as clean and buffered Si.<sup>12</sup> The relatively larger sizes of the triangular mounds (1–2 microns) and the width of terraces (hundreds of nm, see Figure 1(d)) are all indicative of a better quality  $\text{Bi}_2\text{Se}_3$  film grown on InP(111)A by MBE.

In some previous studies of epitaxial  $\text{Bi}_2\text{Se}_3$  on substrates like Si(111), a similarly mounded morphology as that shown in Fig. 1(c) was also noted.<sup>4,12,19</sup> However, there is a distinct difference: the mounds seen in those studies were spirals originated from a preferential growth at screw dislocations.<sup>20</sup> Alternatively, they were created by a mechanism of growth front pinning by jagged steps of the substrate followed by an upward climbing of the growth front over the steps.<sup>19</sup> These spiral mounds are manifested by the winding steps on them, which are easily distinguishable from those seen in Fig. 1(c). Indeed, the mounds on the surface of  $\text{Bi}_2\text{Se}_3$  grown on InP(111)A are of the wedding-cake structure, a morphological feature commonly seen in growth systems dictated by the Ehrlich-Schwoebel (ES) barriers.<sup>21,22</sup> So the wedding-cake mounds in Fig. 1(c) may point to the presence of the ES barrier on  $\text{Bi}_2\text{Se}_3$ (111).

Twin domain suppression in  $\text{Bi}_2\text{Se}_3$ -on-InP(111)A is, in our view, rooted in the 2D step-flow growth mode of  $\text{Bi}_2\text{Se}_3$  on InP(111)A. To show this, Fig. 2 presents a surface after  $\sim 0.1$  quintuple layers (QLs)  $\text{Bi}_2\text{Se}_3$  deposition on an InP(111)A substrate. One notes that the deposits of  $\text{Bi}_2\text{Se}_3$  are mostly aggregated at ascending steps of the substrate, which is characteristic of the step-flow growth process. The lattices of the substrate at steps will then play a guiding role for crystallographic orientation of epitaxial  $\text{Bi}_2\text{Se}_3$ , leading to the single domain film. On a very flat surface containing few steps, epitaxial  $\text{Bi}_2\text{Se}_3$  would proceed by a periodic island nucleation and coalescence, which is manifested by the RHEED intensity oscillations (see inset of Fig. 3(a)). The islands nucleated away from steps are not constraint by the lattices of the substrate at steps, although the hexagonal lattices on flat terraces still provide the epitaxial sites for a crystalline epifilm of  $\text{Bi}_2\text{Se}_3$ . In the growth direction of the  $c$ -axis, there can then be two atomic stacking sequences, one

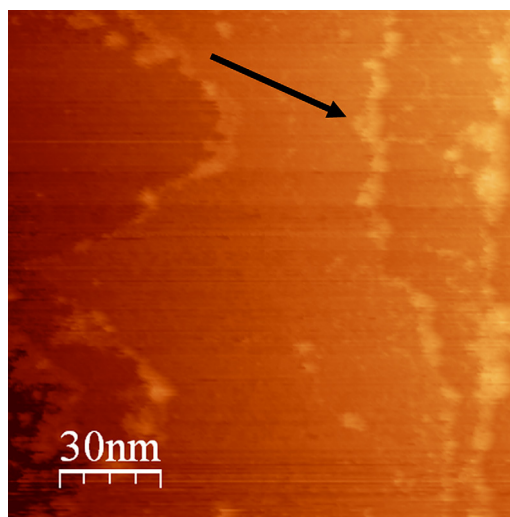


FIG. 2. STM image of a surface following 0.1 QLs  $\text{Bi}_2\text{Se}_3$  deposition on a flat InP(111), where the nucleated islands (arrow pointed, for example) are seen to decorate ascending steps on substrate.

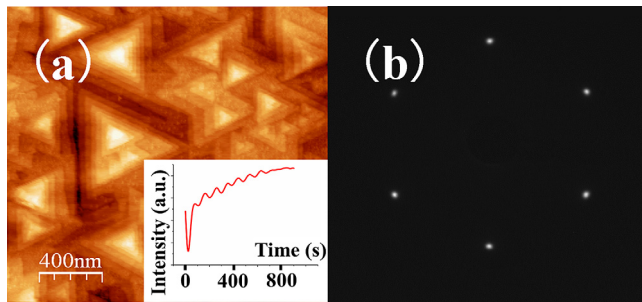


FIG. 3. (a) STM image showing a film of  $\text{Bi}_2\text{Se}_3$  grown on very flat InP substrate via the island nucleation mode, as implied by the RHEED intensity oscillations shown in the inset. (b) The corresponding LEED pattern (taken at 30 eV) showing the six-fold rotation symmetry.

follows that of the substrate, i.e.,  $-\text{[ABC]}_{\text{InP}}-\text{[abcab]}_{\text{Bi}_2\text{Se}_3}$ , and the other is  $60^\circ$  rotated, being  $-\text{[ABC]}_{\text{InP}}-\text{[acbac]}_{\text{Bi}_2\text{Se}_3}$  stacked.<sup>29</sup> If these two stacking sequences are degenerate in energy and thus equally favorable, the epilayer will be twinned. We believe this is exactly the case in the experiment of Fig. 3, where oppositely oriented mounds and six-fold symmetrical LEED patterns signify a twinned film. The lack of  $30^\circ$  rotation domain, on the other hand, affirms the guiding role of the hexagonal lattice of InP(111) surface, which provides the epitaxial sites for epitaxial  $\text{Bi}_2\text{Se}_3$ . To check the two stacking orders are degenerate, we have performed the first principles total energy calculations of one QL  $\text{Bi}_2\text{Se}_3$  on 6 bilayer InP (refer to Fig. 1S in supplementary material<sup>29</sup>) using the Vienna *ab initio* simulation package (VASP).<sup>23</sup> We compared the formation energies of the two configurations and found only a small energy difference ( $\sim 8$  meV per  $1 \times 1$  cell). As it turns out, the rotated domain is slightly more favorable on flat InP(111)A. In practice, real surfaces always contain steps, and if the lattices at the step edges provide additional constraints to the stacking of  $\text{Bi}_2\text{Se}_3$ , the stacking order following the substrate will expectedly become equally or more favorable. Therefore, a competition between the two stacking sequences may lead to twinned films of varying domain sizes on substrates with different step densities.

An important finding from this calculation is that there exists a strong chemical interaction between In and Se atoms at the heterointerface. Specifically, the interaction occurs between the p-orbitals of Se and the  $sp^3$ -orbitals of In atoms.<sup>29</sup> There is a significant overlap in electronic density between the two atoms and their equilibrium distance is about 0.273 nm (see Fig. 4(a)). Meanwhile, the atomic spacing of InP “substrate” near the surface is stretched by the In-Se interaction. For example, the very top layer of In atoms is found to be 0.351 nm above the second indium layer, which amounts to about 0.125 Å expansion over the bulk InP lattice. As a result,  $\text{Bi}_2\text{Se}_3$  growth on InP(111)A does not follow the vdWe process for the first QL, although from the 2nd QL and onwards, it is still of the vdWe process.<sup>16,17</sup> Such a combinational growth kinetics can be beneficial to high quality film growth if the lattice misfit between the substrate and the epilayer is small. It will promote the 2D growth mode due to the lower surface energy of the layered  $\text{Bi}_2\text{Se}_3$  compound than that of the covalent substrate such as InP.<sup>24</sup>

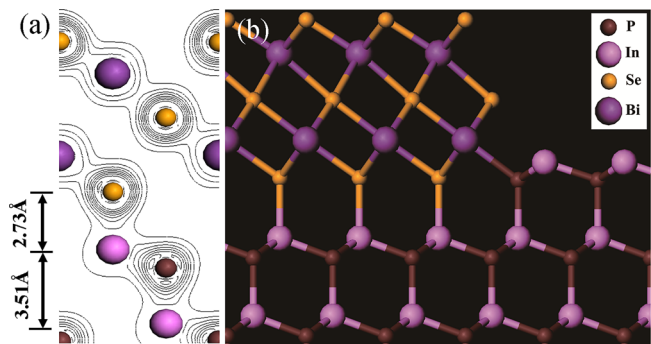


FIG. 4. (a) Electron density map of  $\text{Bi}_2\text{Se}_3$  on a flat InP(111)A obtained from the first principles calculations. (b) Stick-and-ball model illustrating the interface between a stepped InP(111)A substrate and epitaxial  $\text{Bi}_2\text{Se}_3$ , where the chemical interaction between In and Se atoms on the flat terrace and the possible chemical bonding between P and Bi at step edges provide the lattice constraints for a single domain  $\text{Bi}_2\text{Se}_3$  epilayer.

We have also calculated the formation energies of  $\text{Bi}_2\text{Se}_3$  on P-terminated InP(111)B surface. The results suggest that it is less favorable when comparing with InP(111)A surface. The energy difference is about 0.489 eV per ( $1 \times 1$ ) cell. This may reflect the difference in chemical interaction between atoms of Se and In on InP(111)A versus that between Se and P atoms on InP(111)B.

As noted above, the lattice of InP at the surface (interface) layer is considerably stretched from the bulk value when  $\text{Bi}_2\text{Se}_3$  is grown. This lattice expansion is in favor of a possible chemical interaction between P and Bi atoms at steps due to a reduced bond distortion (see Fig. 4(b)). The chemical interaction between P and Bi at steps in turn favors the step-flow mode of growth, making the steps to act as the additional guide to the lattice of epitaxial  $\text{Bi}_2\text{Se}_3$ , suppressing rotation domains in film. Step-flow growth on a stepped InP(111)A is what we have had in the experiment of Figure 1, where the stepped substrate was achieved by the thermal deoxidation procedure. To obtain a flatter surface like the one in Fig. 3, careful and prolonged annealing procedure has to be taken after the thermal deoxidation. An alternative approach to prepare a stepped starting surface is to use a vicinal substrate on which trains of steps are inherently present. We have thus conducted such an experiment using a  $3.5^\circ$  offcut InP(111)A substrate and indeed obtained a single domain film as judged by from the uniform step structure of the surface.<sup>29</sup> We further tested growth on a deliberately roughened InP(111)A where the RHEED pattern was spotty. Obviously on such a surface, no island is expectedly nucleated away from steps. The resulted epilayer was also found to be of single domain.<sup>29</sup> Hence we assert that twin suppression of epitaxial  $\text{Bi}_2\text{Se}_3$  on InP(111)A is due to the step-flow growth mode, where steps of the substrate guide the lattices of epitaxial  $\text{Bi}_2\text{Se}_3$  for a unidirectional film. Selective area transmission electron diffraction and the LEED studies all confirm the lattices of  $\text{Bi}_2\text{Se}_3$  to conform to that of InP substrate with the epitaxial relation of  $\text{Bi}_2\text{Se}_3[111]//\text{InP}[111]$  and  $\text{Bi}_2\text{Se}_3[\bar{1}\bar{1}2]//\text{InP}[\bar{1}\bar{1}2]$ .

From the above analysis, we may suggest similar situations to arise for  $\text{Bi}_2\text{Se}_3$  growth on other III-V substrates, such as GaAs. For the latter, however, large lattice mismatch may cause an ambiguity in growth mode. It will be interesting to examine the growth characteristics of  $\text{Bi}_2\text{Se}_3$  on these other zinc-blende III-V substrates in future studies.

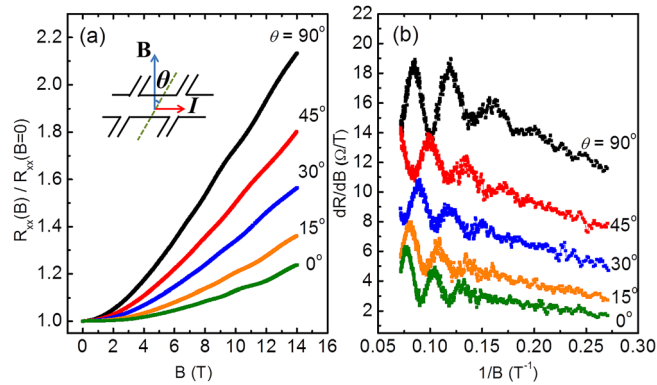


FIG. 5. (a) Normalized magnetoresistance measured at 2 K at different tilted angles  $\theta$  of the B field relative to the film plane as defined in the inset. (b) Derivative magnetoresistance plotted as a function of inverse magnetic field, revealing SdH oscillations at different tilted angles of the B field.

Finally, the electrical properties of  $\text{Bi}_2\text{Se}_3$  grown on  $\text{InP}(111)\text{A}$  are found to be improved over those grown on clean or buffered  $\text{Si}(111)$ , for example. The background doping of  $\sim 1 \times 10^{18} \text{ cm}^{-3}$  and the low-temperature (2 K) electron mobility over  $3500 \text{ cm}^2/\text{V s}$  are derived from low B-field Hall effect measurements, which marks an improvement over the best samples grown on  $\text{Si}(111)$  ( $3.0 \times 10^{18} \text{ cm}^{-3}$  and  $2000 \text{ cm}^2/\text{V s}$ ) but using similar MBE condition.<sup>4,29</sup> Magnetoresistance experiments show SdH oscillations superimposed on a non-saturating linear background as seen in Figure 5(a) for different B-field tilting angles relative to the current and film plane. The non-saturating linear MR is believed to originate from surface states and diminished as the tilting angle is decreased to zero.<sup>25</sup> For each tilting angle, three oscillation periods could be extracted from a plot of derivative magnetoresistance as a function of inverse magnetic field (see Figure 5(b)). However, the oscillation amplitude, phase, and period are different for different tilting angles, indicating that such SdH oscillations contain contributions overwhelmingly from bulk state electrons. The hexagonally deformed anisotropic Fermi surface of  $\text{Bi}_2\text{Se}_3$  (Refs. 26–28) is believed to be responsible for these.

To summarize, we demonstrate the advantages of using  $\text{InP}(111)\text{A}$  as the substrate for epitaxial growth of topological insulator  $\text{Bi}_2\text{Se}_3$ . Particularly, single domain epilayers are consistently obtained by MBE on such a substrate under the step-flow growth mode. Surface steps on the substrate play the guiding role of epitaxial crystallographic orientation, which can be related to a relatively strong chemical interaction between atoms at the heterointerface and steps. The mounded morphology of a thick film suggests an ES-barrier mediated growth process. MR measurements show SdH oscillations at various tilt angles; all show multiple oscillation periods. While the SdH oscillations indicate good quality of the sample, more than one oscillation periods may reflect the anisotropy of the Fermi surface of  $\text{Bi}_2\text{Se}_3$  which requires more in-depth studies.

We are grateful to P. J. Shang and Q. Li for the TEM measurements. Some of the substrate wafers were provided by Y. P. Zeng and Y. W. Zhao at Institute of Semiconductors,

CAS, China. The project was financially supported by the General Research Fund (Nos. 706110, 706111, and 605011) of the Research Grant Council of Hong Kong Special Administrative Region.

<sup>1</sup>Y. Xia, D. Qian, D. Hsieh, L. Wray, A. Pal, H. Lin, A. Bansil, D. Grauer, Y. S. Hor, R. J. Cava, and M. Z. Hasan, *Nat. Phys.* **5**, 398 (2009).

<sup>2</sup>H. J. Zhang, C. X. Liu, X. L. Qi, X. Dai, Z. Fang, and S. C. Zhang, *Nat. Phys.* **5**, 438 (2009).

<sup>3</sup>G. H. Zhang, H. J. Qin, J. Teng, J. D. Guo, Q. L. Guo, X. Dai, Z. Fang, and K. H. Wu, *Appl. Phys. Lett.* **95**, 053114 (2009).

<sup>4</sup>H. D. Li, Z. Y. Wang, X. Kan, X. Guo, H. T. He, Z. Wang, J. N. Wang, T. L. Wong, N. Wang, and M. H. Xie, *New J. Phys.* **12**, 103038 (2010).

<sup>5</sup>A. Richardella, D. M. Zhang, J. S. Lee, A. Koser, D. W. Rench, A. L. Yeats, B. B. Buckley, D. D. Awschalom, and N. Samarth, *Appl. Phys. Lett.* **97**, 262104 (2010).

<sup>6</sup>X. F. Kou, L. He, F. X. Xiu, M. R. Lang, Z. M. Liao, Y. Wang, A. V. Fedorov, X. X. Yu, J. S. Tang, G. Huang, X. W. Jiang, J. F. Zhu, J. Zou, and K. L. Wang, *Appl. Phys. Lett.* **98**, 242102 (2011).

<sup>7</sup>C. L. Song, Y. L. Wang, Y. P. Jiang, Y. Zhang, C. Z. Chang, L. L. Wang, K. He, X. Chen, J. F. Jia, Y. Y. Wang, Z. Fang, X. Dai, X. C. Xie, X. L. Qi, S. C. Zhang, Q. K. Xue, and X. C. Ma, *Appl. Phys. Lett.* **97**, 143118 (2010).

<sup>8</sup>J. Chen, H. J. Qin, F. Yang, J. Liu, T. Guan, F. M. Qu, G. H. Zhang, J. R. Shi, X. C. Xie, C. L. Yang, K. H. Wu, Y. Q. Li, and L. Lu, *Phys. Rev. Lett.* **105**, 176602 (2010).

<sup>9</sup>G. H. Zhang, H. J. Qin, J. Chen, X. Y. He, L. Lu, Y. Q. Li, and K. H. Wu, *Adv. Funct. Mater.* **21**, 2351 (2011).

<sup>10</sup>P. Tabor, C. Keenan, S. Urazdzhin, and D. Lederman, *Appl. Phys. Lett.* **99**, 013111 (2011).

<sup>11</sup>M. H. Liu, C. Z. Chang, Z. C. Zhang, Y. Zhang, W. Ruan, K. He, L. L. Wang, X. Chen, J. F. Jia, S. C. Zhang, Q. K. Xue, X. C. Ma, and Y. Y. Wang, *Phys. Rev. B* **83**, 165440 (2011).

<sup>12</sup>Z. Y. Wang, H. D. Li, X. Guo, W. K. Ho, and M. H. Xie, *J. Cryst. Growth* **334**, 96 (2011).

<sup>13</sup>Y. Takagaki and B. Jenichen, *Semicond. Sci. Technol.* **27**, 035015 (2012).

<sup>14</sup>N. V. Tarakina, S. Schreyeck, T. Borzenko, C. Schumacher, G. Karczewski, K. Brunner, C. Gould, H. Buhmann, and L. W. Molenkamp, *Cryst. Growth Des.* **12**, 1913 (2012).

<sup>15</sup>S. Schreyeck, N. V. Tarakina, G. Karczewski, C. Schumacher, T. Borzenko, C. Brüne, H. Buhmann, C. Gould, K. Brunner, and L. W. Molenkamp, *Appl. Phys. Lett.* **102**, 041914 (2013).

<sup>16</sup>A. Koma, K. Sunouchi, and T. Miyajima, *J. Vac. Sci. Technol. B* **3**, 724 (1985).

<sup>17</sup>A. Koma, *J. Cryst. Growth* **201**, 236 (1999).

<sup>18</sup>M. H. Xie, S. M. Seutter, W. K. Zhu, L. X. Zheng, H. S. Wu, and S. Y. Tong, *Phys. Rev. Lett.* **82**, 2749 (1999).

<sup>19</sup>Y. Liu, M. Weinert, and L. Li, *Phys. Rev. Lett.* **108**, 115501 (2012).

<sup>20</sup>W. K. Burton, N. Cabrera, and F. C. Frank, *Philos. Trans. R. Soc. London, Ser. A* **243**, 299 (1951).

<sup>21</sup>M. D. Johnson, C. Orme, A. W. Hunt, D. Graff, J. Sudijono, L. M. Sander, and B. G. Orr, *Phys. Rev. Lett.* **72**, 116 (1994).

<sup>22</sup>J. A. Strosio, D. T. Pierce, M. D. Stiles, A. Zangwill, and L. M. Sander, *Phys. Rev. Lett.* **75**, 4246 (1995).

<sup>23</sup>G. Kresse and J. Furthmüller, *Phys. Rev. B* **54**, 11169 (1996).

<sup>24</sup>E. Bauer and J. H. Vandermerwe, *Phys. Rev. B* **33**, 3657 (1986).

<sup>25</sup>H. T. He, B. K. Li, H. C. Liu, X. Guo, Z. Y. Wang, M. H. Xie, and J. N. Wang, *Appl. Phys. Lett.* **100**, 032105 (2012).

<sup>26</sup>K. Eto, Z. Ren, A. A. Taskin, K. Segawa, and Y. Ando, *Phys. Rev. B* **81**, 195309 (2010).

<sup>27</sup>K. Kuroda, M. Arita, K. Miyamoto, M. Ye, J. Jiang, A. Kimura, E. E. Krasovskii, E. V. Chulkov, H. Iwasawa, T. Okuda, K. Shimada, Y. Ueda, H. Namatame, and M. Taniguchi, *Phys. Rev. Lett.* **105**, 076802 (2010).

<sup>28</sup>M. Bianchi, D. D. Guan, S. N. Bao, J. L. Mi, B. B. Iversen, P. D. C. King, and P. Hofmann, *Nat. Commun.* **1**, 128 (2010).

<sup>29</sup>See supplementary material at <http://dx.doi.org/10.1063/1.4802797> for models of  $\text{Bi}_2\text{Se}_3$ -on- $\text{InP}(111)\text{A}$ , calculated local density of states, some additional topographic images of  $\text{Bi}_2\text{Se}_3$  grown on vicinal and rough substrates, and the Hall data measured at low-temperature but varying B-fields.